

See discussions, stats, and author profiles for this publication at: <https://www.researchgate.net/publication/281152886>

Laminar Flame Speeds and Kinetic Modeling of n-Pentanol and Its Isomers

ARTICLE *in* ENERGY & FUELS · AUGUST 2015

Impact Factor: 2.79 · DOI: 10.1021/acs.energyfuels.5b00740

READS

38

5 AUTHORS, INCLUDING:



[Qianqian Li](#)

Xi'an Jiaotong University

26 PUBLICATIONS 449 CITATIONS

[SEE PROFILE](#)



[Chenglong Tang](#)

Xi'an Jiaotong University

72 PUBLICATIONS 735 CITATIONS

[SEE PROFILE](#)



[Li Guan](#)

Xi'an Jiaotong University

5 PUBLICATIONS 4 CITATIONS

[SEE PROFILE](#)



[Zuohua Huang](#)

Xi'an Jiaotong University

419 PUBLICATIONS 5,178 CITATIONS

[SEE PROFILE](#)

Laminar Flame Speeds and Kinetic Modeling of *n*-Pentanol and Its Isomers

Qianqian Li, Chenglong Tang, Yu Cheng, Li Guan, and Zuohua Huang*

State Key Laboratory of Multiphase Flow in Power Engineering, Xi'an Jiaotong University, Xi'an, People's Republic of China

S Supporting Information

ABSTRACT: A comprehensive experimental and computational study was conducted on the laminar combustion characteristics and chemical kinetics of four pentanol isomer–air mixtures (*n*-pentanol, 3-methyl-1-butanol, 2-methyl-1-butanol, and 2-methyl-2-butanol). Experiments were performed at the equivalence ratios ranging from 0.6 to 1.8, three initial temperatures (393, 433, and 473 K), and four pressures (0.1, 0.25, 0.5, and 0.75 MPa) using outwardly propagating flames. Results show that the laminar flame speeds of the four pentanol isomers decrease in the order of *n*-pentanol, 2-methyl-1-butanol, 3-methyl-1-butanol, and 2-methyl-2-butanol. The most significant differences among the isomers are observed around the stoichiometric mixture. Simulations on the laminar flame speeds of *n*-pentanol and 3-methyl-1-butanol were respectively performed using the model of Heufer et al. and Sarathy et al. Comparisons between the simulations and experimental data show the *n*-pentanol model yields satisfactory agreement with the data at most conditions but slight overpredictions at rich mixtures and atmospheric pressure and the 3-methyl-1-butanol model yields close agreement with the data at all conditions. For 2-methyl-1-butanol, a model based on the model proposed by Tang et al. was developed and validated against the data of laminar flame speed as well as ignition delay times. Sensitivity analysis indicates that the laminar flame speeds of the isomer–air flames (*n*-pentanol, 3-methyl-1-butanol, and 2-methyl-1-butanol) are mainly sensitive to small molecule reactions involving H₂–O₂ and C₁–C₃ species but not to fuel-specific reactions. The concentrations of H₂–O₂ and C₁–C₃ intermediates are responsible for the laminar flame speed difference among the isomers. Additionally, butene isomers working as the important intermediates occupy different fractions in various pentanol isomer flames, confirming the differences on the chemical structure and the reaction pathways of the isomers.

1. INTRODUCTION

While considerable studies have been conducted on the combustion characteristics of ethanol and butanol for their utility as practical biofuels,^{1–8} the potential of the heavier alcohols, namely, the pentanols, has been recently recognized. Specifically, pentanols have higher energy content, have lower corrosivity, and are less hygroscopic. They can be produced from diverse processes, such as the distillation of fossil oil, fermentation, the terpenoid pathway, and the Fischer–Tropsch process.^{9–12} Furthermore, more efficient and advanced means of engineering-scale production of pentanol are being actively developed, stimulating related research in all aspects.

Research on pentanol combustion and utilization was initiated about 10 years ago, with Gautam et al.^{2,3} studying the combustion and emission characteristics of pentanol/gasoline blends in a single-cylinder engine. Their results showed that, compared to neat gasoline, the blends produce similar cyclic emissions of CO, CO₂, and organic matter hydrocarbon equivalent (OMHCE) but have higher NO_x emission and cycle fuel consumption. Furthermore, the brake specific emissions and brake specific fuel consumption were significantly reduced. Yang et al.¹³ studied 3-methyl-1-butanol (*iso*-pentanol) in an HCCI engine and found it promising, for two reasons. First, its combustion results in considerable intermediate temperature heat release (ITHR) which plays a significant role in reducing knock at high loads dominated by retarded combustion. Second, it shows high HCCI reactivity, as it needs a lower intake temperature than either gasoline or ethanol at the same test condition. Finally, studies on pure *n*-

pentanol and blended *n*-pentanol/diesel in diesel engines showed that the blended fuel exhibits improved combustion characteristics and lower particulate emissions based on both mass and molar concentrations.^{14–16}

In parallel with engine studies, various kinetic models of the pentanol isomers were developed. Such developments, however, have been constrained by the scarcity and lack of comprehensiveness of the data. Specifically, the model of Togbé et al.¹⁷ for *n*-pentanol agreed reasonably well with their experimental data on the stable species measured in a jet-stirred reactor (JSR) over various equivalence ratios ranging from 0.35 to 4.0, at 1.0 MPa, and on laminar flame speeds at 423 K and 0.1 MPa. However, the model did not agree with the laminar flame speeds of Li et al.¹⁸ for lean mixtures at temperatures of 393–473 K and pressures of 0.1–0.75 MPa. The model of Heufer et al.¹⁹ for *n*-pentanol was validated with many sets of experimental data including the laminar flame speeds measured by Togbé et al.,¹⁷ with the result indicating overprediction for rich mixtures. Dayma,²⁰ Tsujimura,²¹ and Sarathy et al.²² subsequently developed models for 3-methyl-1-butanol. Simulations of the first two models were validated with ignition delay and JSR data, while that of Sarathy was tested against various experimental data covering a wide pressure range of 0.1–6.0 MPa, a temperature range of 650–1500 K in both premixed and diffusion environments including one set of laminar flame

Received: April 7, 2015

Revised: July 14, 2015

Published: July 15, 2015

Table 1. Fuel Properties of Pentanol Isomers

Chemical name	Purity	Molecular formula	Structure
<i>n</i> -pentanol(NP)	>99%	C ₅ H ₁₂ O	
3-methyl-1-butanol(3M1B)	>99%	C ₅ H ₁₂ O	
2-methyl-1-butanol(2M1B)	>98%	C ₅ H ₁₂ O	
2-methyl-2-butanol(2M2B)	>99%	C ₅ H ₁₂ O	

speed at 353 K and 0.1 MPa measured by Egolfopoulos and co-workers. Tang et al.²³ proposed a model for 2-methyl-1-butanol validated with shock tube ignition delays. Particularly, Sarathy et al.²⁴ recently reviewed the combustion chemistry of several alcohol fuels, and indicated it is difficult to give comprehensive analysis on pentanol isomers with the rather limited experimental data. In view of the above consideration, additional experimental data are clearly needed to further validate the published models and aid the model development.

The present investigation extends the previous studies^{18,25} on the straight carbon chain of *n*-, 2-, and 3-pentanol isomers and the combustion characteristics of 2-methyl-1-butanol. Specifically, laminar flame speeds of two isomer-air flames (3-methyl-1-butanol and 2-methyl-2-butanol) were acquired from outwardly propagating spherical flames at equivalence ratios of 0.6–1.8, temperatures of 393, 433, and 473 K, and elevated pressures of 0.1, 0.25, 0.5, and 0.75 MPa. For *n*-pentanol and 2-methyl-1-butanol, instead of using the linear fit laminar flame speeds published in previous studies, new values were determined with the nonlinear extrapolation. A comparative study was then conducted on the combustion characteristics and chemical kinetics of four pentanol isomers, namely, *n*-pentanol (NP), 3-methyl-1-butanol (3M1B), 2-methyl-1-butanol (2M1B), and 2-methyl-2-butanol (2M2B). It should be noted that present modeling work is limited to the high temperature combustion chemistry. The models of *n*-pentanol and 3-methyl-1-butanol for simulations, respectively, developed by Heufer et al.¹⁹ and Sarathy et al.,²² were directly used to model the experimental laminar flame speed. The 2-methyl-1-butanol model originally proposed by Tang et al.²³ was refined to achieve improved accuracy. Finally, sensitivity analysis and reaction pathways were conducted to identify the key intermediate species.

2. EXPERIMENTAL SETUP AND DATA PROCESSING

2.1. Experimental Setup. Laminar flame speeds were determined using the constant-volume chamber technique. A detailed description of the experimental setup can be found in previous publications.^{26,27} Briefly, the chamber is cylindrical, with an inner diameter of 180 mm, volume of 5.8 L, and components for heating, ignition, data acquisition, and high-speed schlieren photography. Heating is accomplished by a 1.5 kW heating-tape wrapped outside the chamber. An S type thermocouple with an accuracy of 1 K is mounted in the center of the chamber to calibrate the mixture temperature.

In acquiring the experimental data, at least three experiments were performed for each condition. Properties of the fuels used are listed in Table 1. 21% O₂ and 79% N₂ were, respectively, supplied into the chamber as the dry air through the inlet/outlet valve. The purity of the gas is higher than 99.95%.

2.2. Extraction of Laminar Flame Speeds. The flame radius history was recorded with a schlieren system. Detailed analysis shows

the error of the flame radius measurement is within $\pm 1.35\%$. From the flame radius history, $r_f(t)$, the unstretched flame speed, S_b^0 , can be extracted through the nonlinear expression of Kelley et al.,²⁸ $S_b^0 t + C = r_f + 2L_b \ln r_f - (4L_b^2/r_f) - (8L_b^3/3r_f^2)$, where L_b is the Markstein length of the burned mixture. Finally, the (unburned) laminar flame speed is determined by $S_u^0 = \rho_b^0 S_b^0 / \rho_u$ where ρ_u and ρ_b^0 are the unburned and burned gas densities, respectively.

Various factors need to be taken into account in a high-quality measurement of laminar flame speed which include flame instability,^{29,30} ignition,³¹ chamber confinement,^{32,33} radiation,³⁴ extrapolation method, and mixture preparation.³⁵ The present study has abandoned the data of the flame surface with full-fledged cellular during data extrapolation. It is noted the flame surface is not always smooth and is sometimes populated by large cracks. These are embryonic manifestations of flame front instability, but unlike the full-fledged cellular flames, they are not expected to affect the accuracy of the laminar flame speed determined. To eliminate the effects of the ignition and the chamber confinement, most of the measurements are limited to flame radii of 8–22 mm. Measurements need to be started from a radius larger than 8 mm and ended at a radius smaller than 22 mm with far larger Lewis number.

The radiation effect could modify the flame speed especially near the limits of flammability. Yu et al.³⁴ reported the radiation-induced uncertainty is lower than 5% around the stoichiometric ratio but greater than 5% at extremely lean or rich mixtures. The present experiments extend the initial condition to 1.8, where the radiation effect cannot be neglected. Therefore, the radiation-corrected laminar flame speed will be determined by $S_{u,RCFS}^0 = S_{u,Exp}^0 + 0.82S_{u,Exp}^0(S_{u,Exp}^0/S_0)^{-1.14}(T_u/T_0)(P_u/P_0)^{-0.3}$, where $S_{u,Exp}^0$ is the measured laminar flame speed; $S_0 = 0.01\text{ m}\cdot\text{s}^{-1}$; $T_0 = 298\text{ K}$; $P_0 = 0.1\text{ MPa}$; and T_u and P_u are the initial temperature and initial pressure, respectively.

The uncertainty induced by the flame speed extrapolation method and mixture preparation is included in the total uncertainty. The total uncertainty of laminar flame speed in the present study is estimated with the method of Moffat et al.³⁶ This method has been extensively used to evaluate the experimental uncertainty of laminar flame speed measurement,^{37–39} and is expressed as

$$\delta_{S_u^0} = \sqrt{(B_{S_u^0})^2 + \left(\frac{t_{M-1.95} S_{S_u^0}}{\sqrt{M}}\right)^2} \quad (1)$$

where $B_{S_u^0}$ is the total bias uncertainty of the measurement method, i.e., the accuracy of the outwardly propagating flame method; M are repetitions for each experimental condition; $t_{M-1.95}$ is the student's t distribution with freedom degrees of $M - 1$ and a confidence interval of 95%; and $S_{S_u^0}$ is the standard deviation of S_u^0 at each condition, derived from the laminar flame speeds of repeated experiments. The total bias uncertainty, $B_{S_u^0}$, can be extracted through the equation as follows

$$B_{S_u^0} = \sqrt{\sum_{i=1}^n \left(\frac{\partial S_u^0(x_i)}{\partial x_i} u_i \right)^2} \quad (2)$$

where x_i indicates each factor affecting the determination of laminar flame speed and u_i represents the uncertainty of each factor.

With the experimental data at various initial conditions, laminar flame speed can be correlated with equivalence ratio, initial temperature, and initial pressure through the equation $S_u^0 = S_u^0(\phi)(T_u/T_{u0})^{\alpha_t(\phi)}(P_u/P_{u0})^{\beta_p(\phi)}$, where T_{u0} and P_{u0} respectively indicate the reference temperature and pressure. The details of the correlation can be found in ref 25. The variation of the initial temperature is 393 (433, 473) \pm 2 K; thus, the biggest relative temperature error is \pm 0.5%. The deviation between the initial pressure and the target pressure is \pm 3 kPa; thus, the relative pressure error at normal pressure is \pm 1%. The uncertainty of the equivalence ratio is mainly induced by the measurement errors of the microliter syringes and pressure gauge. The microliter syringes were employed to inject the liquid fuels into the chamber, and the pressure gauge indicates the pressure in the chamber. The uncertainty of the equivalence ratio is estimated to be \pm (2–3)%. This value is not marked in the figures for clarity. With the analysis above, the total bias uncertainty is evaluated to be 1.3–3 $\text{cm}\cdot\text{s}^{-1}$. For each condition, the experiments were repeated three times, and the standard error can be evaluated with the experimental data. Finally, the total experimental uncertainty was estimated to be 2–4 $\text{cm}\cdot\text{s}^{-1}$.

2.3. Reactor Models. The simulations were conducted with the PREMIX code in the CHEMKIN software.^{40,41} The unburned temperature was set to be the initial temperatures of 393, 433, and 473 K. The pressures were 0.1, 0.25, 0.5, and 0.75 MPa. Soret diffusion was included, together with mixture-averaged transport. Simulations were solved with 200 adaptive grid points and 1500 maximum grid points, while the adaptive grid control based on solution curvature and gradient were reduced to 0.06.

Model validation also included the shock tube data on the ignition delays at high temperatures.²³ Simulations of the ignition delay were conducted with the Closed Homogenous Batch Reactor module, employing constant volume and adiabatic system. The end time is set to be 0.1 s, which is greater than the measured ignition delays. The pressure and temperature were given as the experimental conditions. Default absolute and relative tolerances were used in the simulations. The ignition delay was simulated as the time to reach the peak fraction of [OH], and was found to be close to the time of the steepest temperature rise.

3. RESULTS AND DISCUSSION

3.1. Laminar Flame Speeds of the Four Pentanol Isomers. In the present study, the nonlinear methodology was employed to determine the laminar flame speeds of *n*-pentanol and 2-methyl-1-butanol. Figure 1 plots the data of stretched flame speed versus flame radius/stretch rate for pentanol isomer–air mixtures at 1.2, 433 K, and 0.1 MPa. It is seen that the stretched flame speed, S_b , increases with decreasing stretch rate, κ , corresponding to the increasing flame radius. Among the isomer flames, the unstretched flame speed decreases in the order of *n*-pentanol, 2-methyl-1-butanol, 3-methyl-1-butanol, and 2-methyl-2-butanol. When the flame radius approaches infinity, the stretch rate vanishes and thus the unstretched flame speed, S_b^0 , is deduced. Meanwhile, Markstein length, indicating the effect of stretch on the burning intensity of the flame, is also acquired. According to the law of mass conservation on the flame front, laminar flame speed is obtained through $S_u^0 = \rho_b^0 S_b^0 / \rho_u$.

The radiation effect on laminar flame speed is quantitatively determined with the empirical correlation reported by Yu et al.³⁴ Figure 2 shows relative and absolute values of the radiation-induced laminar flame speed reduction (R and A) of *n*-pentanol–air mixtures at different initial temperatures and initial pressures. Obviously, the values of A are all within 1 cm/s , smaller than the experimental uncertainty. The values of R are small at most conditions, however, greater than 5% at the

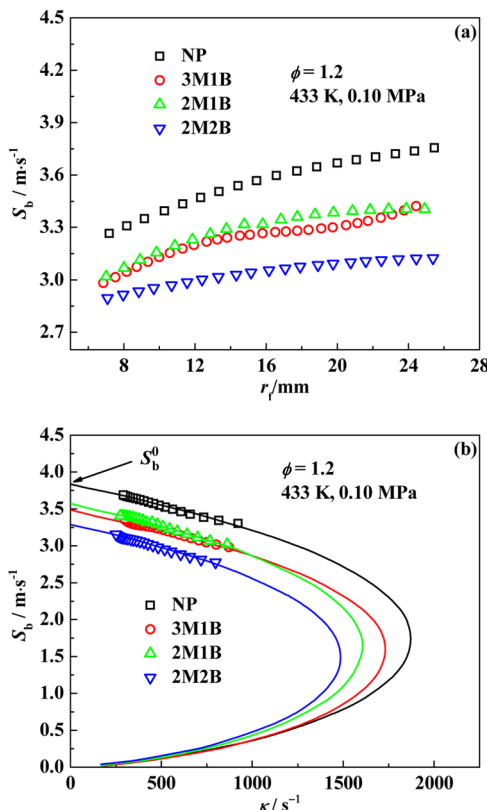


Figure 1. Stretched flame speed versus flame radius/stretch rate at $\phi = 1.2$, 433 K, and 0.1 MPa for pentanol isomer–air mixtures.

extremely rich mixtures of 1.7 and 1.8. Therefore, the laminar flame speeds reported in the present study are all radiation-corrected values.

Figure 3 shows the comparison of laminar flame speeds determined with linear and nonlinear methodologies for *n*-pentanol–air mixtures at various initial conditions, where the linear fit results have been published in a previous study.¹⁸ It should be noted that the linear results were not radiation-corrected values. Obviously, the results yielded in two different ways are approximate at all conditions with a slight difference for lean and rich mixtures. However, the differences between the two groups of data are smaller than 2 $\text{cm}\cdot\text{s}^{-1}$, within the uncertainty of measurements.

Figure 4 presents the Markstein length, L_b , of pentanol isomer–air mixtures at 433 K and 0.1 MPa. It is seen that L_b gradually decreases with the increasing equivalence ratio due to the effect of Lewis number.²⁷ Additionally, it exhibits similar values for pentanol isomer–air mixtures at the fixed equivalence ratio, initial pressure, and initial temperature, indicating the negligible difference of the stretch effect on the isomer flames. Markstein lengths of the isomer–air mixtures at all experimental conditions have been included as Supporting Information.

Figure 5 plots the laminar flame speeds of four pentanol isomer–air mixtures at 433 K and various initial pressures. It is seen that *n*-pentanol has the highest laminar flame speeds for all equivalence ratios, followed by 2-methyl-1-butanol and 3-methyl-1-butanol, and 2-methyl-2-butanol has the lowest values. This order remains for all pressures studied, which also represents the order of high temperature reactivity. The high temperature reactivity characteristic among pentanol isomers indicated by laminar flame speed is consistent with

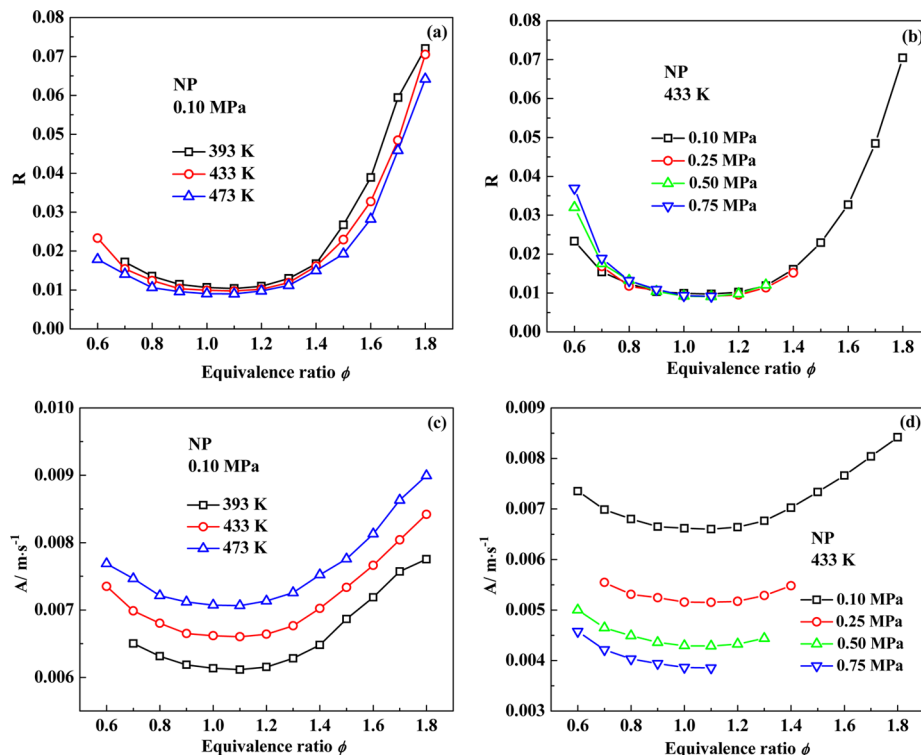


Figure 2. Relative and absolute values of the radiation-induced laminar flame speed reduction (R and A) of *n*-pentanol–air mixtures at different initial temperatures and initial pressures.

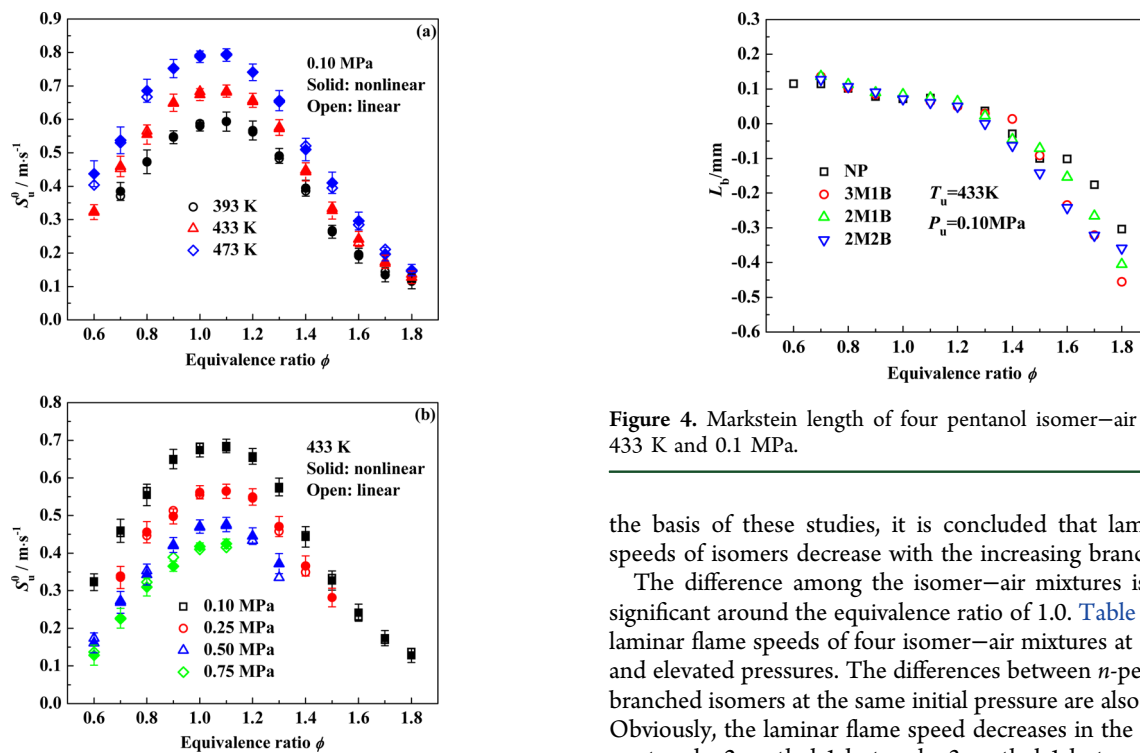


Figure 3. Comparison of the laminar flame speeds determined with linear and nonlinear methodologies for *n*-pentanol–air mixtures at different conditions.

the ignition delay times comparison presented by Tang et al.²³ The fastest flame speeds of primary fuel among fuel isomers were also observed for propanol, butanol, and octane.^{42–44} On

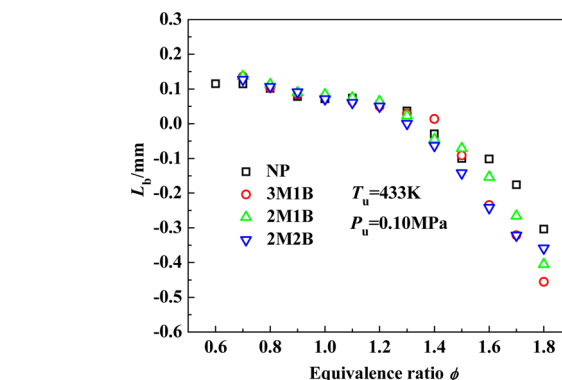


Figure 4. Markstein length of four pentanol isomer–air mixtures at 433 K and 0.1 MPa.

the basis of these studies, it is concluded that laminar flame speeds of isomers decrease with the increasing branch number.

The difference among the isomer–air mixtures is the most significant around the equivalence ratio of 1.0. Table 2 gives the laminar flame speeds of four isomer–air mixtures at 1.0, 433 K, and elevated pressures. The differences between *n*-pentanol and branched isomers at the same initial pressure are also presented. Obviously, the laminar flame speed decreases in the order of *n*-pentanol, 2-methyl-1-butanol, 3-methyl-1-butanol, and 2-methyl-2-butanol. The values of 2-methyl-1-butanol are always higher than those of 3-methyl-1-butanol by 2–3 cm/s at the same initial pressure. With the increase of initial pressure, the difference between *n*-pentanol and 3-methyl-1-butanol increases from 5.78 to 11.48%. Similar behavior is also observed for the other two isomers with the difference respectively increasing from 2.67 to 7.18% between *n*-pentanol and 2-methyl-1-butanol and from 9.05 to 15.55% between *n*-pentanol

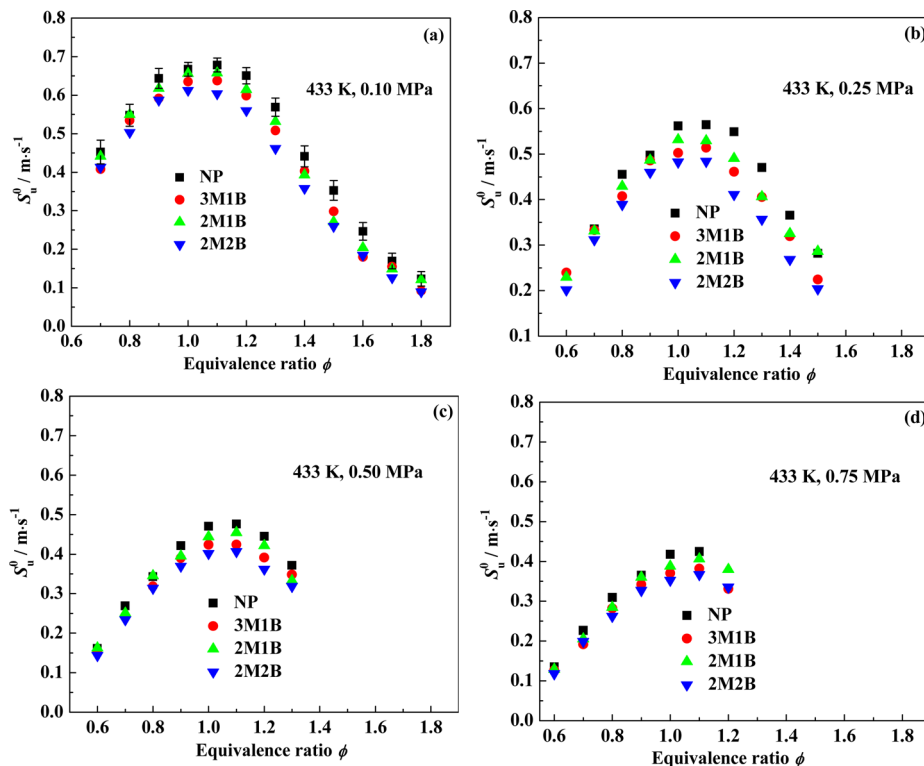


Figure 5. Laminar flame speeds of pentanol isomer–air mixtures versus equivalence ratio at 433 K and different initial pressures. Error bars are plotted just for *n*-pentanol at 0.10 MPa for clarity.

Table 2. Laminar Flame Speeds of Four Isomer–Air Mixtures at 1.0 and 433 K

$\phi = 1.0, T_u = 433 \text{ K}$	$P_u = 0.1 \text{ MPa}$		$P_u = 0.25 \text{ MPa}$		$P_u = 0.5 \text{ MPa}$		$P_u = 0.75 \text{ MPa}$	
	$S_u^0 (\text{m}\cdot\text{s}^{-1})$	deviated from NP						
NP	0.674		0.556		0.471		0.418	
3M1B	0.635	5.78%	0.503	9.53%	0.424	10.09%	0.37	11.48%
2M1B	0.656	2.67%	0.532	4.32%	0.445	5.52%	0.388	7.18%
2M2B	0.613	9.05%	0.483	13.1%	0.402	14.65%	0.353	15.55%

and 2-methyl-2-butanol. This phenomenon was also reported for butanol isomers studied by Wu et al.⁴⁵ but not observed in another butanol isomer study of Gu et al.²⁶ and a butanol–isoctane blending fuel study of Broustail et al.⁴⁶

3.2. Model Validation and Improvement. The experimental data of laminar flame speed were adopted to validate the accuracy of the recently proposed models. Figure 6 plotted the simulated results of two models as well as the experimental data obtained by different groups. All data were measured with spherical propagating flame covering the temperatures of 393–473 K and pressures of 0.1–0.75 MPa. The set of data at 423 K and 0.1 MPa was measured by Togbé et al.,¹⁷ and the rest of the data were obtained in the present study. It is seen that the data of Togbé et al.¹⁷ at 423 K are higher than the present data at 393 K for lean mixtures but approximate the data at 393 K for rich mixtures. At all conditions, the laminar flame speed acquires the peak value between 1.0 and 1.1. Regarding the two models used for simulations, one model (NUI model) was proposed by Heufer et al.¹⁹ Another one (XJTU model)¹⁸ was the modified version of the model proposed by Togbé et al.¹⁷ As shown in Figure 6a and b, the NUI model yields fairly good agreement with the experimental data at most initial conditions but slightly overpredicts the data at rich mixtures and normal pressure. The deviations between the simulations and

experimental data are much more significant at 423 K. As shown in Figure 6c and d, the XJTU model well predicts the results at 423 K over the whole equivalence ratio range. When it was validated against present data, good agreement was obtained for rich mixtures while underestimations were presented for lean mixtures.

Both of the models have been validated against JSR data in the previous studies with good agreements.^{17–19} To further evaluate the prediction ability, the models are also validated with ignition delay times.²³ Figure 7a plots the comparison between the ignition delay times and computed values at 0.1 MPa, 5% *n*-pentanol ratio, and different equivalence ratios. Both models yield satisfactory agreement at $\phi = 0.25$. At $\phi = 0.5$, the NUI model well predicts the experimental data at high temperatures but yields overpredictions at relatively low temperatures. The XJTU model overestimates the experimental data over the whole temperature range. For $\phi = 1.0$, deviations between simulations and experimental data are presented for both models but are bigger for the XJTU model, which remains at a high pressure, as shown in Figure 7b. According to the comparisons between various experimental data sets and model simulation results, the NUI model is adopted to do the further analysis.

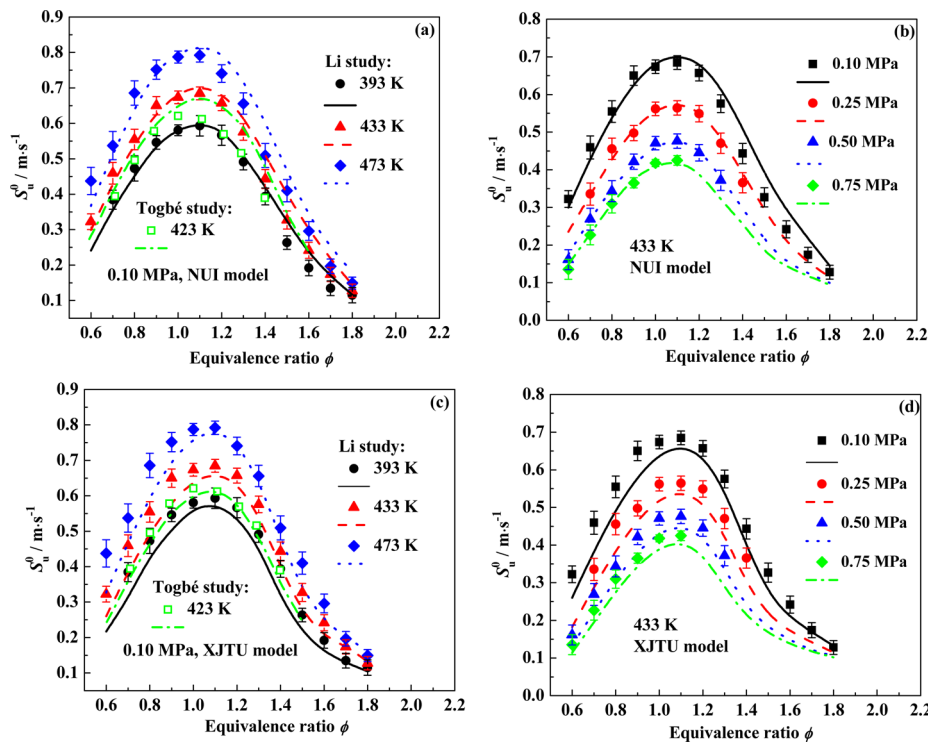


Figure 6. Comparison between the experimental results of *n*-pentanol and the simulation results of two different models respectively developed by Li et al.¹⁸ and Heufer et al.¹⁹

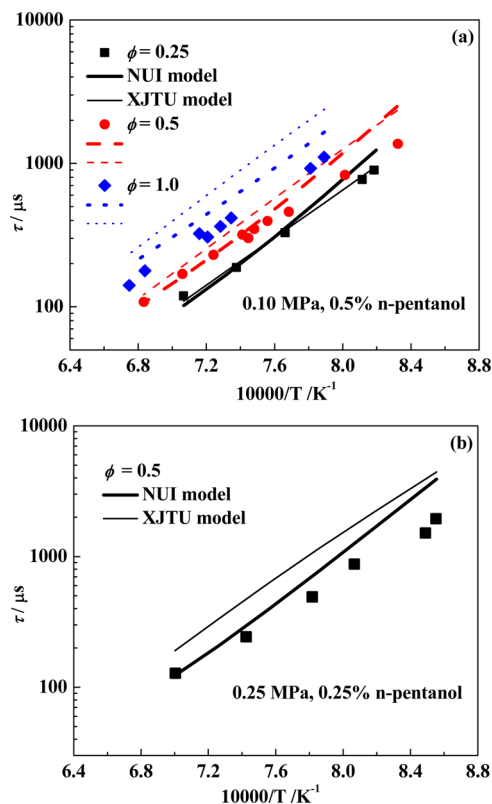


Figure 7. Comparison between the model simulation results and the experimental results for *n*-pentanol. (Two models used for the simulation are the NUI model¹⁹ and the XJTU model.¹⁸)

Figure 8 shows the comparison between the measured and computed laminar flame speeds for 3-methyl-1-butanol–air mixtures. The model applied

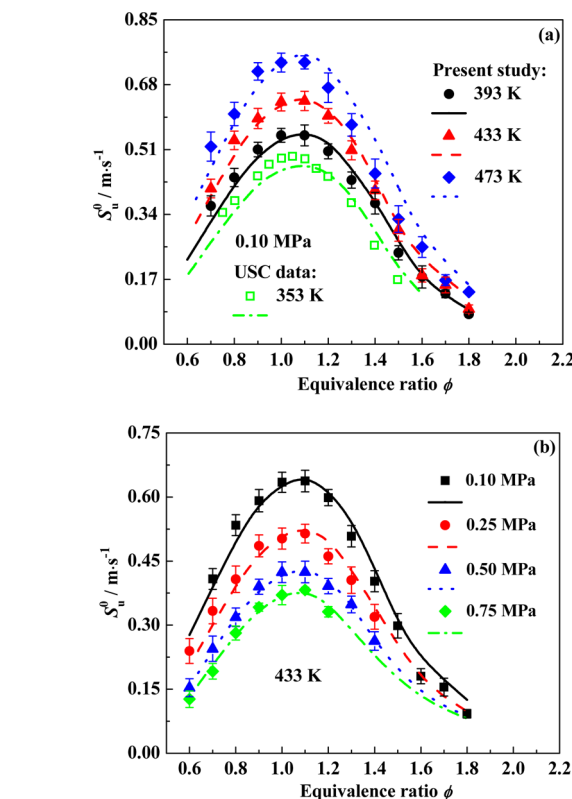


Figure 8. Comparison of the simulations with the experimental results of 3-methyl-1-butanol–air mixtures. The model used for simulation is proposed by Sarathy et al.²²

for simulations was proposed by Sarathy et al.,²² and named the CCRC model in the present study. This model has been validated with the laminar flame speeds obtained by the USC

Table 3. New Calculated Transport Properties with RMG Software

species	chemical formula	geometry	ε/k_B	σ	μ	α	Z_{rot}
butoh2m	CH ₃ CH ₂ CH(CH ₃)CH ₂ OH	2	303.884	6.281	0	0	1
but2m-1	CH ₃ CH ₂ C(CH ₃)CH ₃	2	334.296	5.744	0	0	1
but2m1d	CH ₃ CH ₂ C(CH ₃)=CH ₂	2	340.579	5.705	0	0	1
butoh2m-1	CH ₃ CH ₂ CH(CH ₃)CHOH	2	300.371	6.211	0	0	1
butoh2m-2	CH ₃ CH ₂ C(CH ₃)CH ₂ OH	2	300.371	6.211	0	0	1
butoh2m-3	CH ₃ CHCH(CH ₃)CH ₂ OH	2	300.371	6.211	0	0	1
butoh2m-4	CH ₂ CH ₂ CH(CH ₃)CH ₂ OH	2	300.371	6.211	0	0	1
butoh2m-5	CH ₃ CH ₂ CH(CH ₂)CH ₂ OH	2	300.371	6.211	0	0	1
buto2m	CH ₃ CH ₂ CH(CH ₃)CH ₂ O	2	300.371	6.211	0	0	1
butal2m	CH ₃ CH ₂ CH(CH ₃)CHO	2	346.411	5.969	0	0	1
butal2m-1	CH ₃ CH ₂ CH(CH ₃)CO	2	343.234	5.901	0	0	1
butal2m-2	CH ₃ CH ₂ C(CH ₃)CHO	2	343.234	5.901	0	0	1
butal2m-3	CH ₃ CHCH(CH ₃)CHO	2	343.234	5.901	0	0	1
butal2m-4	CH ₂ CH ₂ CH(CH ₃)CHO	2	343.234	5.901	0	0	1
butal2m-5	CH ₃ CH ₂ CH(CH ₂)CHO	2	343.234	5.901	0	0	1
butoh2m1d3	CH ₃ CHC(=CH ₂)CH ₂ OH	2	313.097	6.098	0	0	1
butoh2m1d	CH ₃ CH ₂ C(CH ₃)=CHOH	2	316.724	6.168	0	0	1
butoh2m4d3	CH ₃ CHC(=CH ₂)CH ₂ OH	2	313.097	6.098	0	0	1
butoh2m13d	CH ₂ =CHC(CH ₃)=CHOH	2	322.013	6.037	0	0	1
butoh2m3d	CH ₂ =CHCH(CH ₃)CH ₂ OH	2	308.829	6.149	0	0	1
butoh2m2d	CH ₃ CH=C(CH ₃)CH ₂ OH	2	316.724	6.168	0	0	1
c4h712ch2oh	CH ₃ CH ₂ C(=CH ₂)CH ₂ OH	2	307.606	6.161	0	0	1
ch3cchoh	CH ₃ C=CHOH	2	300.783	5.377	0	0	1
c4h4oh13-2	CH ₂ =CHC=CHOH	2	308.477	5.618	0	0	1
c5h7-2	CH ₂ =CHC(CH ₃)=CH	2	346.876	5.564	0	0	1

group at 353 K with counterflow flame, and the validation is given in Figure 8 as well for the clarity of comparison with the present data. We see the model yields reasonable agreement with most of the data but underestimates the USC data at equivalence ratios smaller than 1.2. Additionally, the USC data at 353 K is significantly smaller than the present data at 393 K due to the lower initial temperature.

For 2-methyl-1-butanol, Tang et al.²³ from our group proposed a high temperature model which was validated against the ignition delay times at temperatures of 1150–1600 K and pressures of 0.1–0.25 MPa.²³ However, the transport properties of species were absent. In the present study, a file containing the transport parameters of all species is included in the model and this model is defined as the original model. The transport parameters of most species were from the other models,^{47,48} while the rest of the 25 species were estimated with RMG software (Reaction Mechanism Generator) developed by the Green group at MIT.⁴⁹ The new calculated transport parameters are listed in Table 3. Figure 9 gives the comparison between the simulations of the original model and the experimental data. It is seen that the original model well predicts the experimental data at fuel-lean mixtures, while it exhibits higher values at fuel-rich mixtures for all temperatures and pressures. Thus, further improvements are necessary.

To find out the fundamental reasons, we conducted the sensitivity analysis to identify the highly sensitive reactions to laminar flame speed. The normalized sensitivity analysis coefficient k_i is defined as $k_i = (A_i/S_u^0)(\partial S_u^0/\partial A_i)$, where A_i is the reaction rate of reaction i . Sensitivity analysis was respectively conducted for fuel-lean, stoichiometric, and fuel-rich mixtures, as shown in Figure 10. It is seen that the laminar flame speed of 2-methyl-1-butanol is sensitive to small molecule reactions without fuel-specific reactions included. The original 2-methyl-1-butanol model was built on the basis of the n -

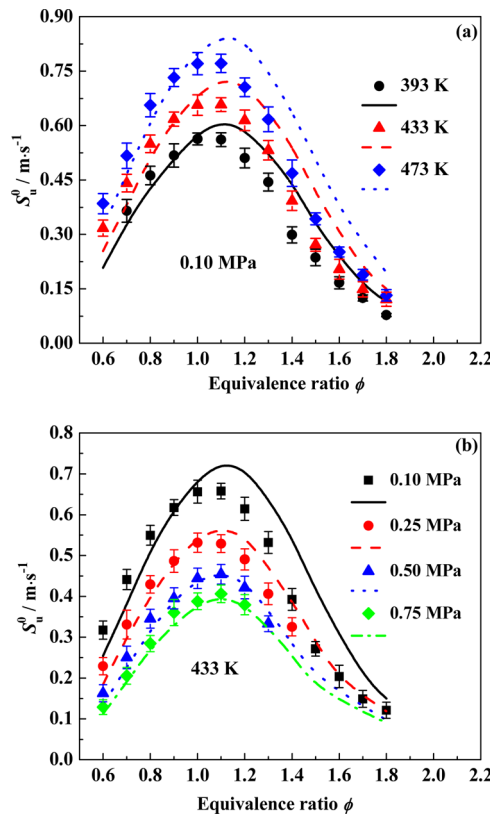


Figure 9. Comparison between the simulated laminar flame speeds of the original model and the nonlinear fit results for 2-methyl-1-butanol–air mixtures.

butanol model,⁴⁷ in which the small molecule reaction mechanism has been developed for several years. Recently,

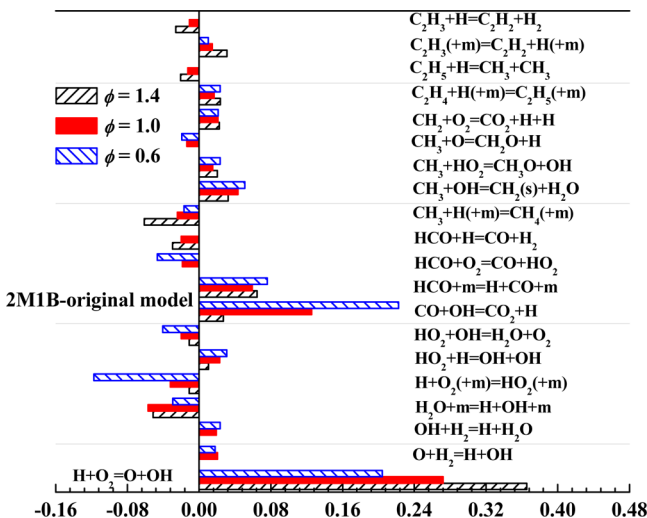


Figure 10. Normalized rate constant sensitivity coefficient on laminar flame speed for 2-methyl-1-butanol at 0.1 MPa and 433 K. The model used for the sensitivity analysis is the original model which was initially proposed by Tang et al.²³

the small molecule model was greatly improved along with new models^{19,22} proposed for *n*-pentanol and 3-methyl-1-butanol. Therefore, the original 2-methyl-1-butanol model is refined through updating all the small molecule submodels of H_2/O_2 and C_1-C_3 with the same part in the *n*-pentanol model.¹⁹ We define this updated model as the modified model, and the kinetic files are provided as Supporting Information.

Figure 11 plots the simulation results of the original and modified models and experimental data at elevated temperatures and pressures for 2-methyl-1-butanol–air mixtures. Compared to the original model, the modified model yields better agreement with the experimental data at fuel-rich mixtures, especially at higher pressures of 0.50 and 0.75 MPa. Besides, reasonable agreement is maintained for fuel-lean mixtures. The models are validated with the ignition delay times²³ as well. As indicated in Figure 12, the modified model yields more accurate predictions than the original model does at all conditions. Specifically, the modified model almost reproduces the ignition delay curve at a pressure of 0.25 MPa and 0.25% *n*-pentanol fuel ratio. The results above not only indicate the high accuracy of the modified model of 2-methyl-1-butanol but also suggest the significant role of the small molecule reactions in the high temperature chemistry kinetics.

Park et al.⁵⁰ recently proposed a model of 2-methyl-1-butanol which was validated against various experimental data sets. This model was built in a similar manner as the NUI model of *n*-pentanol¹⁹ and the CCRC model of 3-methyl-1-butanol,²² and the three models own the same small molecule submodel of C_0-C_3 as well as the modified model of 2-methyl-1-butanol. Simulations of different 2-methyl-1-butanol models are plotted in Figure 13a. Obviously, the modified model exhibits approximate simulation results with Park's model. This result confirms the significant role of the small molecule submodel in the high temperature chemistry. Besides, new data of laminar flame speeds were presented by Park et al.⁵⁰ and are also adopted to validate the modified model of 2-methyl-1-butanol, as indicated in Figure 13b. It is seen that the modified model well predicts the experimental data at all conditions. There is no low temperature chemistry involved in the present study; thus, it is reasonable to use the modified model to

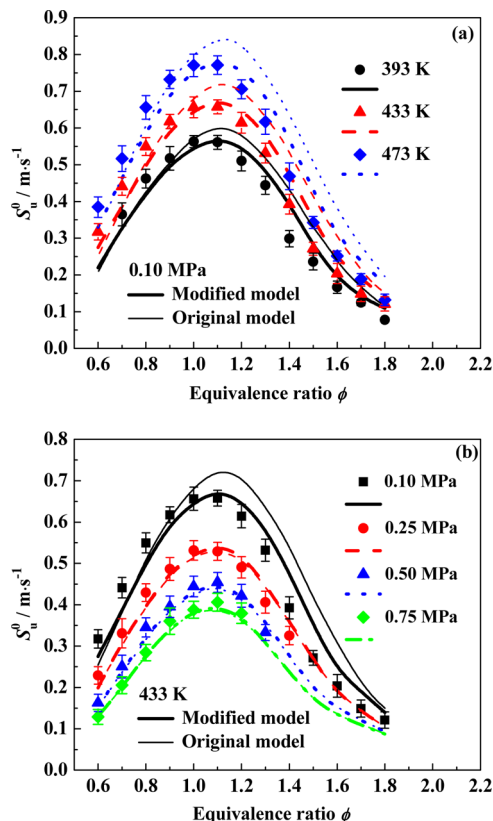


Figure 11. Comparison between simulated laminar flame speeds of the modified model and the nonlinear fit results for 2-methyl-1-butanol.

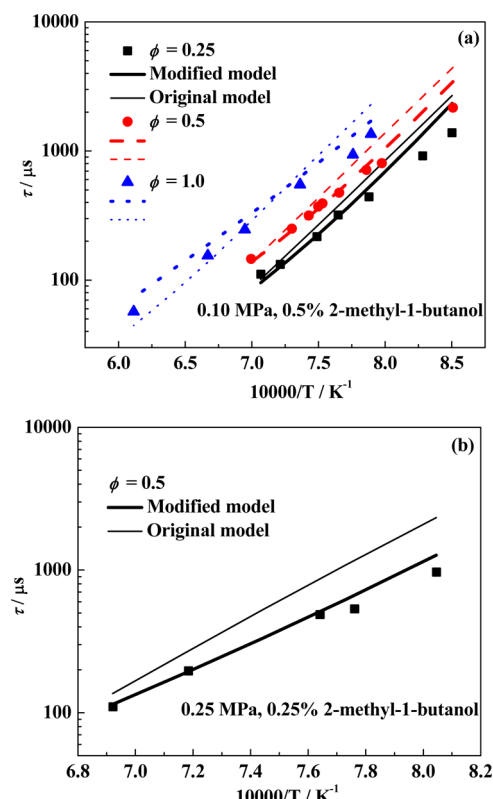


Figure 12. Comparison of simulated ignition delays with the modified model and measured data for 2-methyl-1-butanol. (Bold line, modified model; normal line, original model).

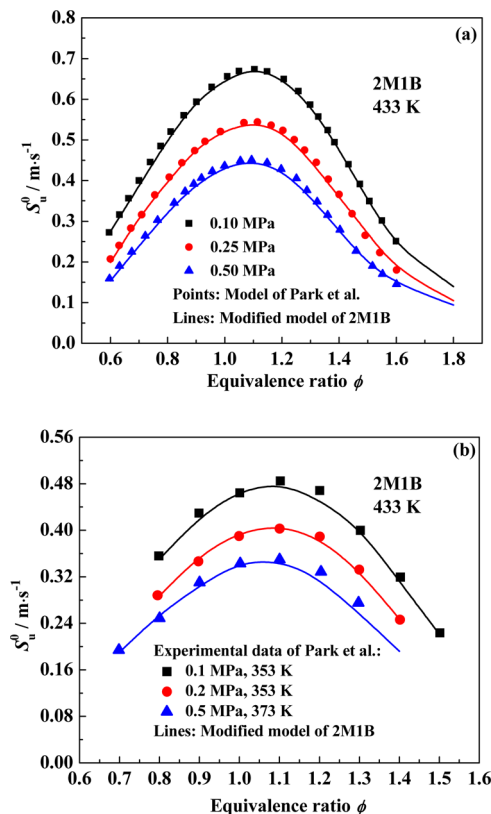


Figure 13. Comparison between simulation results of different models and between simulation results and experimental data measured by Park et al. at different initial conditions.

interpret the differences among pentanol isomer flames in the following analysis.

3.3. Discussions on the Differences among Pentanol Isomer–Air Mixtures. Laminar flame speed differences among isomer flames are mainly determined by two factors, namely, the thermal and chemical kinetic effects.⁴⁵ Figure 14

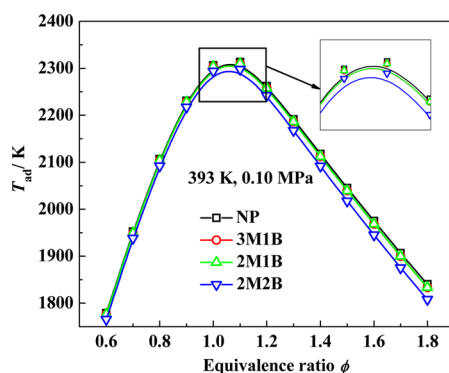


Figure 14. Adiabatic temperature versus equivalence ratio at 393 K and 0.1 MPa.

plots the adiabatic temperature, T_{ad} , versus the equivalence ratio at 393 K and 0.1 MPa. It is observed that all of the curves reach the peaks at an equivalence ratio between 1.0 and 1.1, just as the other heavy hydrocarbon and alcohol fuels.^{26,43,44,51,52} T_{ad} of the four isomers have the approximate values at lean mixtures. For rich mixtures with an equivalence ratio varying from 1.0 to 1.8, T_{ad} of 2-methyl-2-butanol is lower than *n*-pentanol by 13–33 K. The low T_{ad} of 2-methyl-2-butanol will

decrease the whole reaction rate and result in the low flame speed. However, the T_{ad} values of *n*-pentanol, 3-methyl-1-butanol, and 2-methyl-1-butanol are close; thus, the thermal effect is not the main reason causing the flame speed difference.

In the aspect of chemical kinetics, bond energy was used to analyze the flame speed difference among butanol isomers by Gu et al.²⁶ who indicated isomers with more methyl groups have lower laminar flame speeds due to the high energy of the C–H bond in the methyl group. This conclusion can be applied on pentanol isomers as well. *N*-Pentanol has one methyl group and hence the fastest flame speed. 2-Methyl-1-butanol and 3-methyl-1-butanol all have two methyl groups and exhibit lower flame speed. 2-Methyl-2-butanol has three methyl groups and exhibits the lowest flame speed. However, the difference between 2-methyl-1-butanol and 3-methyl-1-butanol cannot be explained, which indicates more knowledge of chemical kinetics is needed.

Figure 15 plots the sensitivity analysis for *n*-pentanol, 3-methyl-1-butanol, and 2-methyl-1-butanol at 0.1 MPa, 433 K, and equivalence ratios of 0.7, 1.0, and 1.4. All of the models involved in the present study are listed in **Table 4**, and the three models used for analysis are the NUI model of *n*-pentanol,¹⁹ the CCRC model²² of 3-methyl-1-butanol, and the modified model of 2-methyl-1-butanol. As expected, the laminar flame speeds of three isomers are all sensitive to the same chain branching reaction, $\text{H} + \text{O}_2 \rightleftharpoons \text{O} + \text{OH}$, and terminal reaction, $\text{CH}_3 + \text{H} (+\text{M}) \rightleftharpoons \text{CH}_4 (+\text{M})$, because of their importance for most hydrocarbon fuels. In addition, the laminar flame speed is largely sensitive to small molecule reactions of H_2/CO and C_1-C_3 reactions. Most of the reactions are the same for the three pentanol isomers just differentiated in the magnitude of sensitivity coefficients. Regarding the rest of the reactions, comparative analysis shows that the laminar flame speed of *n*-pentanol is sensitive to the chain branching reaction $\text{HCCO} + \text{O}_2 \rightleftharpoons \text{CO}_2 + \text{CO} + \text{H}$, which increases the concentration of radical H and promotes the whole reaction and hence accelerates the flame speed, while this reaction is not among the sensitive reactions of 3-methyl-1-butanol and 2-methyl-1-butanol. Meanwhile, laminar flame speeds of 3-methyl-1-butanol and 2-methyl-1-butanol are all sensitive to the OH consuming reaction $\text{C}_3\text{H}_6 + \text{OH} \rightleftharpoons \text{C}_3\text{H}_5\text{-A} + \text{H}_2\text{O}$ which retards the overall reaction rate and decreases the flame speed, and this reaction is not among the sensitive reactions of *n*-pentanol. The sensitivity analysis not only reveals the key species in terms of formation and consumption but also indicates the distributions on species concentrations are varied in the isomer flames. These species concentrations are directly responsible for the difference among the laminar flame speeds of pentanol isomers.

Figure 16 plots the mole fractions of H and O radicals versus distance in pentanol isomer flames at 1.0, 433 K, and 0.1 MPa. Being the most important radicals in the chain branching reactions, the mole fractions of H and O radicals represent the overall reaction rate and flame speed to some extent. The mole fractions of H and O radicals are the largest in the *n*-pentanol flame, referring to the highest flame speed of *n*-pentanol among the isomers. **Figure 17** depicts the mole fraction profiles of methyl (CH_3) and vinyl (C_2H_3) radicals. CH_3 radical is primarily generated from the unimolecular decomposition of heavy species like hydroxypentyl, pentoxy, etc., as shown in **Figure 19**. The mole fraction of CH_3 is the highest in the 3-methyl-1-butanol flame with approximate fractions in *n*-pentanol and 2-methyl-1-butanol flames. CH_3 always undergoes

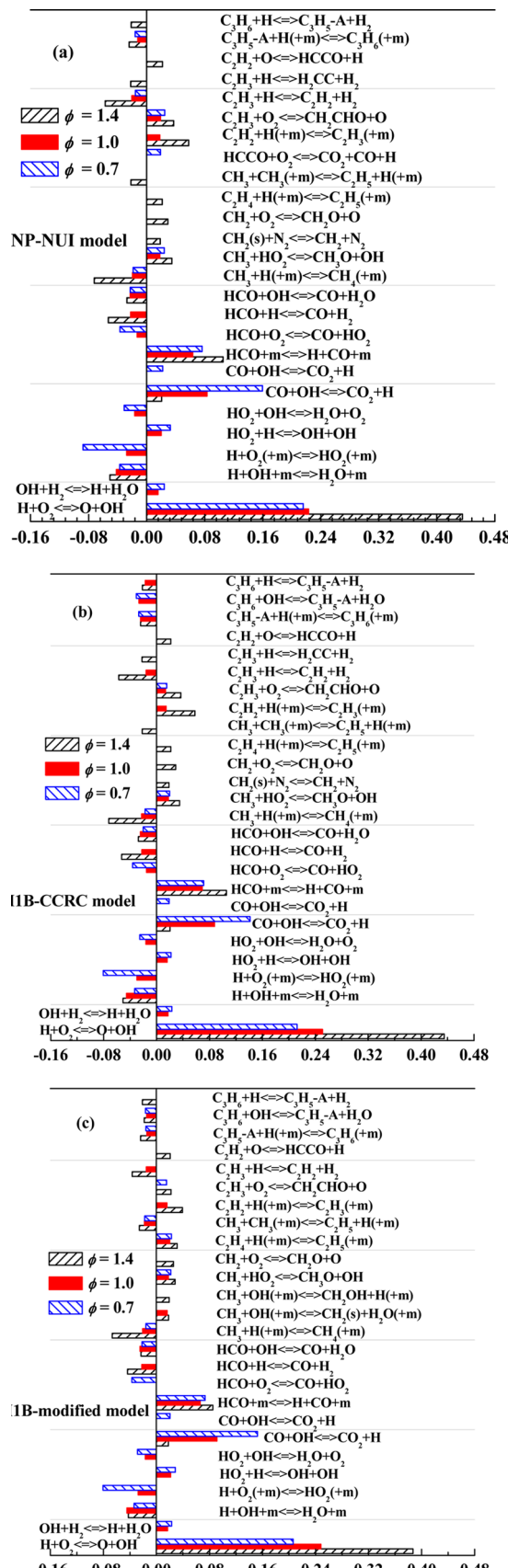


Figure 15. Sensitivity analysis of *n*-pentanol, 3-methyl-1-butanol, and 2-methyl-1-butanol at different equivalence ratios, 0.1 MPa, and 433 K.

Table 4. Models Involved in the Present Study

fuels	models	annotation
<i>n</i> -pentanol	XJTU model	ref 18
	NUI model	ref 19
3-methyl-1-butanol	CCRC model	ref 22
2-methyl-1-butanol	Tang's model	ref 23
	original model	present study based on Tang's model
	modified model	present study
	Park's model	ref 49

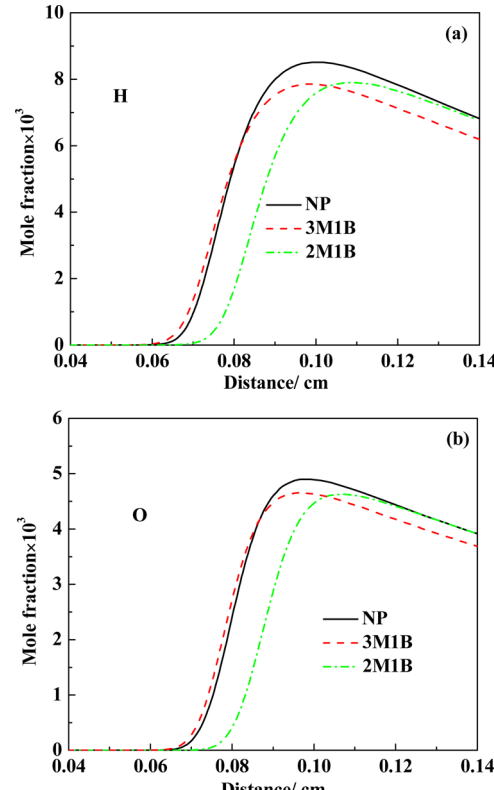


Figure 16. Mole fractions of H and O radicals at $\phi = 1.0$, 433 K, and 0.1 MPa for three isomer flames.

the chain terminating reaction, $\text{CH}_3 + \text{H} \rightleftharpoons \text{CH}_4$, consuming H radicals and inhibiting the flame propagation, which is responsible for the low flame speed of 3-methyl-1-butanol. The mole fractions of C_2H_3 in 3-methyl-1-butanol and 2-methyl-1-butanol flames are almost and roughly half of that in *n*-pentanol flame. Sensitivity analysis indicates that C_2H_3 is mainly produced from the H abstraction of C_2H_4 with C_2H_4 always showing a high concentration in the primary fuel flame. C_2H_3 is consumed through three reactions, $\text{C}_2\text{H}_3 (+m) \rightleftharpoons \text{C}_2\text{H}_2 + \text{H} (+m)$, $\text{C}_2\text{H}_3 + \text{O}_2 \rightleftharpoons \text{CH}_2\text{CHO} + \text{O}$, and $\text{C}_2\text{H}_3 + \text{H} = \text{C}_2\text{H}_2 + \text{H}_2$. Obviously, even though H radical is consumed by the chain-terminating reaction, H, O, and C_2H_2 are all highly reactive radicals which will accelerate the overall reaction rate.

Laminar flame speeds of pentanol isomer-air mixtures are sensitive to some C_3 reactions. As shown in Figure 15, $\text{C}_3\text{H}_5\text{-A}$ is mainly consumed through the chain termination reaction, $\text{C}_3\text{H}_5\text{-A} + \text{H} (+M) = \text{C}_3\text{H}_6 (+M)$, and produced through two ways, $\text{C}_3\text{H}_6 + \text{OH} \rightleftharpoons \text{C}_3\text{H}_5\text{-A} + \text{H}_2\text{O}$ and $\text{C}_3\text{H}_6 + \text{H} \rightleftharpoons \text{C}_3\text{H}_5\text{-A} + \text{H}_2$, which also work as the consumption ways of C_3H_6 . The three reactions are all termination reactions consuming radicals H and OH, exhibiting strong negative sensitivity to the laminar

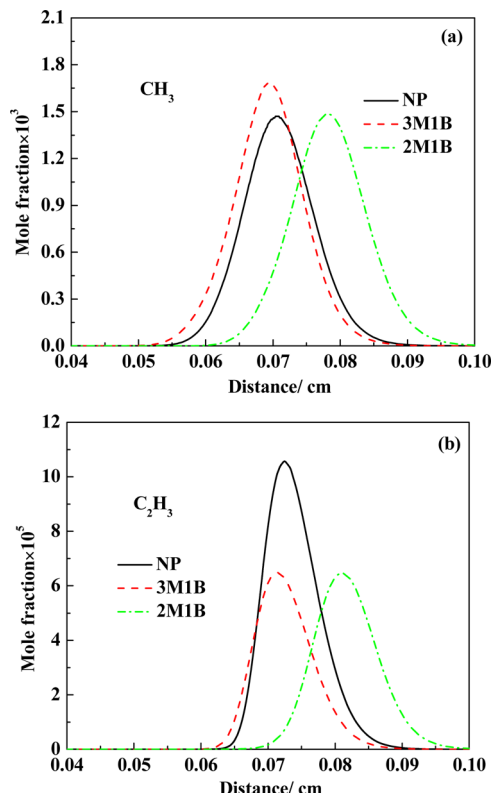


Figure 17. Mole fractions of CH_3 and C_2H_3 at $\phi = 1.0$, 433 K, and 0.1 MPa for three isomer flames.

flame speed. Thus, the high concentrations of $\text{C}_3\text{H}_5\text{-A}$ and C_3H_6 are obstacles in the reaction and flame propagation, which has been proved to be one important reason for the lower flame speed of *iso*-propanol than *n*-propanol.⁴² Figure 18 depicts the profiles of $\text{C}_3\text{H}_5\text{-A}$ and C_3H_6 of three pentanol isomers. Results show the fractions of $\text{C}_3\text{H}_5\text{-A}$ and C_3H_6 in the 3-methyl-1-butanol flame are twice of those in *n*-pentanol–air and 2-methyl-1-butanol–air flames, even though 3-methyl-1-butanol and 2-methyl-1-butanol flames are sensitive to the same C_3 reactions. The different concentrations of C_3 species largely contribute to the differences among the flame speeds of pentanol isomer flames.

Species involved in the sensitive reactions like C_2 and C_3 molecules are all produced through the unimolecular decompositions of the hydroxypentyl and pentyloxy radicals. To further investigate the difference among the isomers, the reaction flux pathway is depicted in Figure 19 at 1.0, 433 K, and 0.1 MPa. It is seen the isomers are all initially consumed by H abstractions from different carbon positions, resulting in various hydroxypentyl and pentyloxy radicals with six productions for *n*-pentanol and 3-methyl-1-butanol and five productions for 2-methyl-1-butanol. More than 30% pentanol is consumed through H abstraction reactions from α -carbon, and less than 2% pentanol is abstracted H from hydroxyl group. Similar results were reported for the other alcohols^{22,43,53} because of the low energy of the C–H bond of α -carbon and the very high energy of the O–H bond. These hydroxyl pentyl and pentyloxy radicals subsequently decompose to be various olefins, aldehydes, alkyl radicals, and smaller hydroxyalkyls through β -scission. Part of the alkyl radicals undergo further scission to form the small alkyl radicals, while the others are consumed to be the relevant olefins which are stable species retarding the

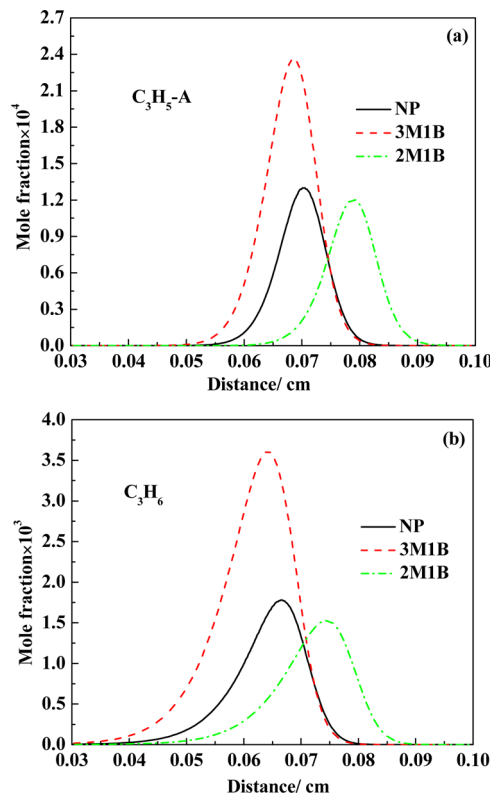


Figure 18. Mole fractions of $\text{C}_3\text{H}_5\text{-A}$ and C_3H_6 at $\phi = 1.0$, 433 K, and 0.1 MPa for three isomer flames.

overall reaction. Comparing the reaction pathways of three pentanol isomers, it is revealed that three butene isomers ($\text{C}_4\text{H}_8\text{-1}$, $i\text{C}_4\text{H}_8$, $\text{C}_4\text{H}_8\text{-2}$) produced from decomposition reactions of hydroxypentyl or butyl radicals ($\text{C}_4\text{H}_9\text{-1}$, $i\text{C}_4\text{H}_9$, $\text{C}_4\text{H}_9\text{-2}$) work as important intermediates in the isomer flames. In the laminar flames, butene isomers are relatively stable species reacting with activated radicals via $\text{C}_4\text{H}_8 + (\text{H}, \text{OH}) \rightleftharpoons \text{C}_4\text{H}_7 + (\text{H}_2, \text{H}_2\text{O})$ and forming C_4H_7 . In the case of $\text{C}_4\text{H}_8\text{-1}$, the production is $\text{C}_4\text{H}_7\text{-1}$ undergoing the decomposition reactions and generating C_2H_3 , C_2H_4 , and C_2H_5 , which are all highly reactive species promoting the whole reaction and flame speed. Evidently, the mole fraction of $\text{C}_4\text{H}_8\text{-1}$ in Figure 20a decreases in the order of *n*-pentanol, 2-methyl-1-butanol, and 3-methyl-1-butanol, consistent with the result of laminar flame speed. The production of *iso*-butene, $i\text{C}_4\text{H}_7$, will persistently react with H/OH, producing a reasonably stable molecule like $\text{H}_2/\text{H}_2\text{O}$ as well as decomposing to be CH_3 simultaneously. All of those species will inhibit the whole reaction and ultimately decrease the laminar flame speed. In Figure 20b, $i\text{C}_4\text{H}_7$ has a rather high concentration in the 3-methyl-1-butanol flame, thus retarding the flame speed. In the case of $\text{C}_4\text{H}_8\text{-2}$ generated from $\text{C}_4\text{H}_8\text{-2}$, the decomposition productions include both the reaction promoted species C_2H_3 and C_2H_4 and the reaction inhibited species CH_3 and C_3H_6 . Therefore, the high concentration of $\text{C}_4\text{H}_8\text{-2}$ in 2-methyl-1-butanol flame, as shown in Figure 20c, contributes to the laminar flame speed little. This reactivity difference between butene isomers was also confirmed by Zhao et al. conducted with laminar flame speed and counterflow ignition.⁵⁴

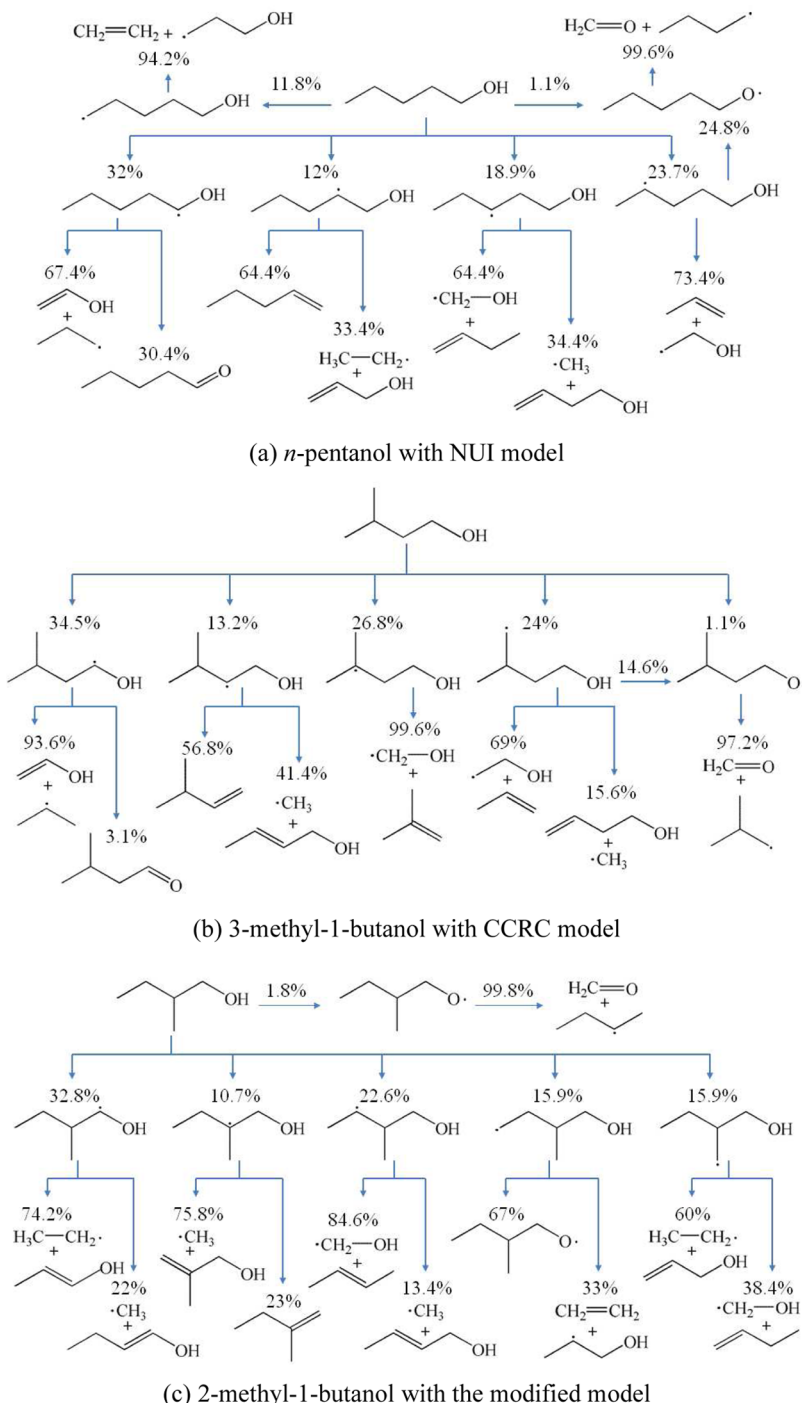


Figure 19. Reaction pathway of three pentanol isomers at $\phi = 1.0$, 433 K, and 0.1 MPa.

4. CONCLUSIONS

A kinetic model and fundamental laminar combustion study were comparatively conducted on four pentanol isomers (*n*-pentanol, 2-methyl-1-butanol, 3-methyl-1-butanol, and 2-methyl-2-butanol) over a wide temperature and pressure range. The laminar flame speeds of four isomer-air mixtures were extracted with a nonlinear relationship from the radius history of the spherical propagating flame. Simulations were developed with the recently proposed models of *n*-pentanol and 3-methyl-1-butanol and the modified model of 2-methyl-1-butanol. Finally, sensitivity analysis and reaction pathways were

depicted with the key species and reactions revealed. The main conclusions are summarized as follows:

- (1) Laminar flame speeds of pentanol isomer-air mixtures decrease in the order of *n*-pentanol > 2-methyl-1-butanol > 3-methyl-1-butanol > 2-methyl-2-butanol. The difference between *n*-pentanol and the other three isomers increases with the increase of initial pressure.
- (2) The *n*-pentanol model proposed by Heufer et al. well predicts the data at most conditions but gives slight underpredictions for rich mixtures and 0.1 MPa. The 3-methyl-1-butanol model developed by Sarathy et al. yields reasonable agreement with the laminar flame speed

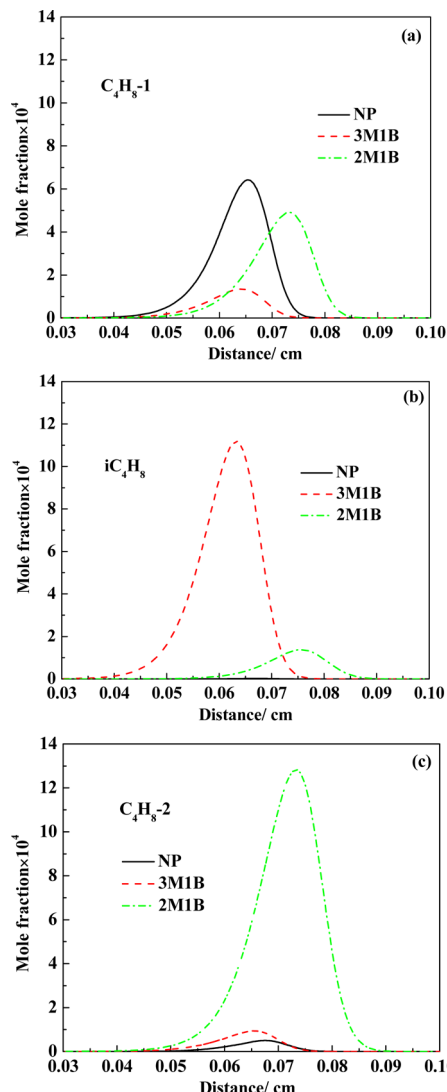


Figure 20. Mole fractions of $C_4H_8\text{-}1$, iC_4H_8 , and $C_4H_8\text{-}2$ at $\phi = 1.0$, 433 K, and 0.1 MPa for three isomer flames.

- measured in the present study at all temperatures and pressures. The modified model of 2-methyl-1-butanol shows better agreement with the data than the original model does through the validations against the experimental data of both laminar flame speeds and high temperature ignition delays.
- (3) Sensitivity analysis indicates the laminar flame speeds of three pentanol isomer–air mixtures (*n*-pentanol, 3-methyl-1-butanol, and 2-methyl-1-butanol) are highly sensitive to a bunch of reactions involving $H_2\text{--O}_2$ and $C_1\text{--C}_3$ species. Most of the reactions are the same just with a difference in the magnitude of the sensitivity coefficients, resulting in different concentrations of key intermediates. Reaction promoting species always have high concentrations in the *n*-pentanol flame. Butene isomers are important intermediates produced in three pentanol isomers with different concentrations. *N*-Butene is mainly produced in the *n*-pentanol flame, 2-butene in the 2-methyl-1-butanol flame, and *iso*-butene in the 3-methyl-1-butanol flame. Concentrations of butene isomers reveal essential differences in chemical structures and reaction pathways among pentanol isomers.

ASSOCIATED CONTENT

Supporting Information

Laminar flame speeds of pentanol isomer–air mixtures at different initial temperatures and initial pressures (efSb00740_si_004.pdf), Markstein length of pentanol isomer–air mixtures at different initial temperatures and initial pressures (efSb00740_si_005.pdf), original data of stretched flame speed versus stretch rate at 433 K and different initial pressures (efSb00740_si_006.pdf), and three kinetic files of the modified model of 2-methyl-1-butanol (txt). The Supporting Information is available free of charge on the ACS Publications website at DOI: [10.1021/acs.energyfuels.Sb00740](https://doi.org/10.1021/acs.energyfuels.Sb00740).

AUTHOR INFORMATION

Corresponding Author

*Phone: 0086 29 82665075. Fax: 0086 29 82668789. E-mail: zhuang@mail.xjtu.edu.cn.

Notes

The authors declare no competing financial interest.

ACKNOWLEDGMENTS

This work is supported by the National Natural Science Foundation of China (Grant Nos. 51406159, 91441203, and 50876085), the National Basic Research Program (2013CB228406), the China Postdoctoral Science Foundation (2014M560774), and State Key Laboratory of Engines, Tianjin University (K2015-01).

REFERENCES

- Dagaut, P.; Togbé, C. Oxidation kinetics of butanol-gasoline surrogate mixtures in a jet-stirred reactor: Experimental and modeling study. *Fuel* **2008**, *87* (15–16), 3313–3321.
- Gautam, M.; Martin, D. W., II. Combustion characteristics of higher-alcohol/gasoline blends. *Proc. Inst. Mech. Eng., Part A* **2000**, *214*, 497–511.
- Gautam, M.; Martin, D. W., II; Carder, D. Emissions characteristics of higher alcohol/gasoline blends. *Proc. Inst. Mech. Eng., Part A* **2000**, *214* (2), 165–182.
- Jin, C.; Yao, M.; Liu, H.; Lee, C.-f. F.; Ji, J. Progress in the production and application of n-butanol as a biofuel. *Renewable Sustainable Energy Rev.* **2011**, *15* (8), 4080–4106.
- Karavalakis, G.; Durbin, T. D.; Shrivastava, M.; Zheng, Z.; Villela, M.; Jung, H. Impacts of ethanol fuel level on emissions of regulated and unregulated pollutants from a fleet of gasoline light-duty vehicles. *Fuel* **2012**, *93* (1), 549–558.
- Koc, M.; Sekmen, Y.; Topgul, T.; Yucesu, H. S. The effects of ethanol-unleaded gasoline blends on engine performance and exhaust emissions in a spark-ignition engine. *Renewable Energy* **2009**, *34* (10), 2101–2106.
- Ozsezen, A. N.; Canakci, M. Performance and combustion characteristics of alcohol-gasoline blends at wide-open throttle. *Energy* **2011**, *36* (5), 2747–2752.
- Yucesu, H. S.; Topgul, T.; Cinar, C.; Okur, M. Effect of ethanol-gasoline blends on engine performance and exhaust emissions in different compression ratios. *Appl. Therm. Eng.* **2006**, *26* (17–18), 2272–2278.
- Cann, A. F. BIOT 80—Production of 2-methyl-1-butanol in engineered *Escherichia coli*. *Abstr. Pap. Am. Chem.* **2009**, 238.
- Cann, A. F.; Liao, J. C. Production of 2-methyl-1-butanol in engineered *Escherichia coli*. *Appl. Microbiol. Biotechnol.* **2008**, *81* (1), 89–98.
- Cann, A. F.; Liao, J. C. Pentanol isomer synthesis in engineered microorganisms. *Appl. Microbiol. Biotechnol.* **2010**, *85* (4), 893–899.

- (12) Connor, R.; Liao, J. Microbial production of advanced transportation fuels in nonnatural hosts. *Curr. Opin. Biotechnol.* **2009**, *20* (3), 307–315.
- (13) Yang, Y.; Dec, J. E.; Dronniou, N.; Simmons, B. Characteristics of isopentanol as a fuel for HCCI engines. *SAE Int. J. Fuels Lubricants* **2010**, *3* (2), 725–741.
- (14) Campos-Fernandez, J.; Arnal, J. M.; Gomez, J.; Lacalle, N.; Dorado, M. P. Performance tests of a diesel engine fueled with pentanol/diesel fuel blends. *Fuel* **2013**, *107* (0), 866–872.
- (15) Li, L.; Wang, J.; Wang, Z.; Liu, H. Combustion and emissions of compression ignition in a direct injection diesel engine fueled with pentanol. *Energy* **2015**, *80* (0), 575–581.
- (16) Wei, L.; Cheung, C. S.; Huang, Z. Effect of n-pentanol addition on the combustion, performance and emission characteristics of a direct-injection diesel engine. *Energy* **2014**, *70* (0), 172–180.
- (17) Togbé, C.; Halter, F.; Foucher, F.; Mounaim-Rousselle, C.; Dagaut, P. Experimental and detailed kinetic modeling study of 1-pentanol oxidation in a JSR and combustion in a bomb. *Proc. Combust. Inst.* **2011**, *33*, 367–374.
- (18) Li, Q.; Hu, E.; Zhang, X.; Cheng, Y.; Huang, Z. Laminar flame speeds and flame instabilities of pentanol isomer-air mixtures at elevated temperatures and pressures. *Energy Fuels* **2013**, *27* (2), 1141–1150.
- (19) Heufer, K. A.; Sarathy, S. M.; Curran, H. J.; Davis, A. C.; Westbrook, C. K.; Pitz, W. J. Detailed Kinetic Modeling Study of n-Pentanol Oxidation. *Energy Fuels* **2012**, *26* (11), 6678–6685.
- (20) Dayma, G.; Togbé, C.; Dagaut, P. Experimental and detailed kinetic modeling study of isoamyl alcohol (Isopentanol) oxidation in a jet-stirred reactor at elevated pressure. *Energy Fuels* **2011**, *25* (11), 4986–4998.
- (21) Tsujimura, T.; Pitz, W. J.; Gillespie, F.; Curran, H. J.; Weber, B. W.; Zhang, Y.; Sung, C. J. Development of isopentanol reaction mechanism reproducing autoignition character at high and low temperatures. *Energy Fuels* **2012**, *26* (8), 4871–4886.
- (22) Sarathy, S. M.; Park, S.; Weber, B. W.; Wang, W.; Veloo, P. S.; Davis, A. C.; Togbé, C.; Westbrook, C. K.; Park, O.; Dayma, G.; Luo, Z.; Oehlschlaeger, M. A.; Egolfopoulos, F. N.; Lu, T.; Pitz, W. J.; Sung, C.-J.; Dagaut, P. A comprehensive experimental and modeling study of iso-pentanol combustion. *Combust. Flame* **2013**, *160* (12), 2712–2728.
- (23) Tang, C.; Wei, L.; Man, X.; Zhang, J.; Huang, Z.; Law, C. K. High temperature ignition delay times of C5 primary alcohols. *Combust. Flame* **2013**, *160* (3), 520–529.
- (24) Sarathy, S. M.; Oßwald, P.; Hansen, N.; Kohse-Höinghaus, K. Alcohol combustion chemistry. *Prog. Energy Combust. Sci.* **2014**, *44* (0), 40–102.
- (25) Li, Q.; Hu, E.; Cheng, Y.; Huang, Z. Measurements of laminar flame speeds and flame instability analysis of 2-methyl-1-butanol-air mixtures. *Fuel* **2013**, *112* (0), 263–271.
- (26) Gu, X. L.; Huang, Z. H.; Wu, S.; Li, Q. Q. Laminar burning velocities and flame instabilities of butanol isomers-air mixtures. *Combust. Flame* **2010**, *157* (12), 2318–2325.
- (27) Tang, C.; Huang, Z.; Jin, C.; He, J.; Wang, J.; Wang, X.; Miao, H. Explosion characteristics of hydrogen–nitrogen–air mixtures at elevated pressures and temperatures. *Int. J. Hydrogen Energy* **2009**, *34* (1), 554–561.
- (28) Kelley, A. P.; Smallbone, A. J.; Zhu, D. L.; Law, C. K. Laminar flame speeds of C5 to C8 n-alkanes at elevated pressures: Experimental determination, fuel similarity, and stretch sensitivity. *Proc. Combust. Inst.* **2011**, *33* (1), 963–970.
- (29) Bradley, D.; Lawes, M.; Liu, K.; Verhelst, S.; Woolley, R. Laminar burning velocities of lean hydrogen–air mixtures at pressures up to 1.0 MPa. *Combust. Flame* **2007**, *149* (1–2), 162–172.
- (30) Jomaas, G.; Law, C. K.; Bechtold, J. K. On transition to cellularity in expanding spherical flames. *J. Fluid Mech.* **2007**, *583*, 1–26.
- (31) Kim, H. H.; Won, S. H.; Santner, J.; Chen, Z.; Ju, Y. Measurements of the critical initiation radius and unsteady propagation of n-decane/air premixed flames. *Proc. Combust. Inst.* **2013**, *34* (1), 929–936.
- (32) Bonhomme, A.; Selle, L.; Poinsot, T. Curvature and confinement effects for flame speed measurements in laminar spherical and cylindrical flames. *Combust. Flame* **2013**, *160* (7), 1208–1214.
- (33) Chen, Z.; Burke, M. P.; Ju, Y. Effects of compression and stretch on the determination of laminar flame speeds using propagating spherical flames. *Combust. Theory Modell.* **2009**, *13* (2), 343–364.
- (34) Yu, H.; Han, W.; Santner, J.; Gou, X.; Sohn, C. H.; Ju, Y.; Chen, Z. Radiation-induced uncertainty in laminar flame speed measured from propagating spherical flames. *Combust. Flame* **2014**, *161* (11), 2815–2824.
- (35) Chen, Z. On the accuracy of laminar flame speeds measured from outwardly propagating spherical flames: Methane/air at normal temperature and pressure. *Combust. Flame* **2015**, *162* (6), 2442–2453.
- (36) Moffat, R. J. Describing the uncertainties in experimental results. *Exp. Therm. Fluid Sci.* **1988**, *1* (1), 3–17.
- (37) Lowry, W.; de Vries, J.; Krejci, M.; Petersen, E.; Serinyel, Z.; Metcalfe, W.; Curran, H.; Bourque, G. Laminar flame speed measurements and modeling of pure alkanes and alkane blends at elevated pressures. *J. Eng. Gas Turbines Power* **2011**, *133* (9), 091501.
- (38) Krejci, M. C.; Mathieu, O.; Vissotski, A. J.; Ravi, S.; Sikes, T. G.; Petersen, E. L.; Kéromnès, A.; Metcalfe, W.; Curran, H. J. Laminar flame speed and ignition delay time data for the kinetic modeling of hydrogen and syngas fuel blends. *J. Eng. Gas Turbines Power* **2013**, *135* (2), 021503.
- (39) Zhang, Y.; Shen, W.; Fan, M.; Zhang, H.; Li, S. Laminar flame speed studies of lean premixed H₂/CO/air flames. *Combust. Flame* **2014**, *161* (10), 2492–2495.
- (40) Kee, R. J.; Grcar, J. F.; Smooke, M. D.; Miller, J. A. PRMIX: a FORTRAN program for modeling steady laminar one-dimensional premixed flames Sandia National Laboratory, 1985, SAND Report 85-8240.
- (41) Kee, R. J.; Rupley, F. M.; Miller, J. A. CHEMKIN-II: a Fortran chemical kinetics package for the analysis of gas-phase chemical kinetics. Sandia National Laboratory, 1989, Technical Report SAND89-8009.
- (42) Veloo, P. S.; Egolfopoulos, F. N. Studies of n-propanol, iso-propanol, and propane flames. *Combust. Flame* **2011**, *158* (3), 501–510.
- (43) Veloo, P. S.; Egolfopoulos, F. N. Flame propagation of butanol isomers/air mixtures. *Proc. Combust. Inst.* **2011**, *33*, 987–993.
- (44) Ji, C. S.; Sarathy, S. M.; Veloo, P. S.; Westbrook, C. K.; Egolfopoulos, F. N. Effects of fuel branching on the propagation of octane isomers flames. *Combust. Flame* **2012**, *159* (4), 1426–1436.
- (45) Wu, F.; Law, C. K. An experimental and mechanistic study on the laminar flame speed, Markstein length and flame chemistry of the butanol isomers. *Combust. Flame* **2013**, *160* (12), 2744–2756.
- (46) Broustail, G.; Halter, F.; Seers, P.; Moréac, G.; Mounain-Rousselle, C. Experimental determination of laminar burning velocity for butanol/iso-octane and ethanol/iso-octane blends for different initial pressures. *Fuel* **2013**, *106*, 310–317.
- (47) Black, G.; Curran, H. J.; Pichon, S.; Simmie, J. M.; Zhukov, V. Bio-butanol: Combustion properties and detailed chemical kinetic model. *Combust. Flame* **2010**, *157* (2), 363–373.
- (48) Curran, H. J.; Gaffuri, P.; Pitz, W. J.; Westbrook, C. K. A comprehensive modeling study of iso-octane oxidation. *Combust. Flame* **2002**, *129* (3), 253–280.
- (49) Green, W. H.; Allen, J. W.; Ashcraft, R. W.; Beran, G. J.; Goldsmith, C. F.; Harper, M. R.; Jalan, A.; Magoon, G. R.; Matheu, D. M.; Petway, S.; Raman, S.; Sharma, S.; Van Geem, K. M.; Song, J.; Wen, J. P.; West, R. H.; Wong, A.; Wong, H.-W.; Yelvington, P. E.; Yu, J. RMG - Reaction Mechanism Generator v3.3. <http://rmg.sourceforge.net/>, 2012.
- (50) Park, S.; Manna, O.; Khaled, F.; Bougacha, R.; Mansour, M. S.; Farooq, A.; Chung, S. H.; Sarathy, S. M. A comprehensive experimental and modeling study of 2-methylbutanol combustion. *Combust. Flame* **2015**, *162* (5), 2166–2176.
- (51) Bradley, D.; Hicks, R. A.; Lawes, M.; Sheppard, C. G. W.; Woolley, R. The measurement of laminar burning velocities and Markstein numbers for iso-octane-air and iso-octane-n-heptane-air

mixtures at elevated temperatures and pressures in an explosion bomb. *Combust. Flame* **1998**, *115* (1–2), 126–144.

(52) Broustail, G.; Seers, P.; Halter, F.; Moreac, G.; Mounaim-Rousselle, C. Experimental determination of laminar burning velocity for butanol and ethanol iso-octane blends. *Fuel* **2011**, *90* (1), 1–6.

(53) Sarathy, S. M.; Vranckx, S.; Yasunaga, K.; Mehl, M.; Osswald, P.; Metcalfe, W. K.; Westbrook, C. K.; Pitz, W. J.; Kohse-Hoinghaus, K.; Fernandes, R. X.; Curran, H. J. A comprehensive chemical kinetic combustion model for the four butanol isomers. *Combust. Flame* **2012**, *159* (6), 2028–2055.

(54) Zhao, P.; Yuan, W.; Sun, H.; Li, Y.; Kelley, A. P.; Zheng, X.; Law, C. K. Laminar flame speeds, counterflow ignition, and kinetic modeling of the butene isomers. *Proc. Combust. Inst.* **2015**, *35* (1), 309–316.